Available online at http://www.journalcra.com

International Journal of Current Research
Vol. 9, Issue, 05, pp.51423-51429, May, 2017

INTERNATIONAL JOURNAL OF CURRENT RESEARCH

ISSN: 0975-833X

RESEARCH ARTICLE

MODELING AND QUANTIFYING THE DETECTION THRESHOLDS OF FLUOROCHROMES PAIRED WITH A MOLECULAR PROBE OF INTEGRINS REGARDING THE DEVELOPMENT OF AN IMAGING STRATEGY FOR THE LYMPH NODE INVOLVEMENT

***,[1]BADIANE S. Moussa, [2]SOBILO Julien, [2]RAES Florian, [2]LERONDEL Stéphanie, [3]N'DOYE Oumar, [1]DIAGNE Ibrahima and [2,4]LE PAPE Alain**

[1]Faculty of Health Sciences /University Gaston Berger of Saint-Louis, Senegal
[2]TAAM UPS44, CIPA, CNRS, Orleans, France, Centre for Small Animal Imaging - Orléans, France
[3]Faculty of Health Sciences, UCAD, Dakar, Senegal
[4]INSERM U1100 - CEPR, Study Center for Respiratory Diseases- Tours, France

ARTICLE INFO

Article History:
Received 13th February, 2017
Received in revised form
15th March, 2017
Accepted 18th April, 2017
Published online 31st May, 2017

Key words:

Sentinel lymph nodes,
integrin targeting,
RGD,
Fluorescence imaging.

ABSTRACT

The concept of sentinel lymph nodes in oncological surgery is based on the fact that the spread of solid tumors in an orderly manner passes first through the lymphatic system. Thus, the sentinel lymph node, meaning the first lymph node encountered by lymphatic drainage from the site of the tumor, is likely to be the first one affected by metastasis. Therefore, a negative sentinel lymph node makes it very unlikely that other lymph nodes along the same lymphatic pathway will be affected. Our interest in the development of an alternative molecular imaging technique for the localization and the detection of the sentinel lymph node micro-invasion is highly triggered by the limits of the current techniques. In this context, RGD mimetic molecular probes are prime targets for fluorescence invivo imaging. The work we report here consist in validating the detection of a fluorochrome paired with a mime RGD from the lymph nodes collected ex vivo. In a translational research approach, we have chosen as animal model some healthy sheep lymph nodes. For the various intra-ganglionic fluorochromes tested, AF750-RGD could be used to give good fluorescence signal from the 1/100 dilution, i.e. 10 nmol, and this fluorescence increases with the concentration of AF750-RGD. For the Cy5.5 the net fluorescence signal appears only from the dilution 1/20 i.e. 5nmol and intensifies with dilution 1/10. Finally, for the ICG (Indo Cyanine Green), a good fluorescence signal is obtained with respect to the sample at the dilution 1/500, i.e. 7.75 mmol. However the unmixing spectral, better than the subtraction of background noise, improves the contrast. Validation of these detection thresholds from these lymph nodes directs us on the choice of fluorochromes and their concentration in a targeting strategy of integrins by fluorescence imaging.

Citation: BADIANE S. Moussa, SOBILO Julien, RAES Florian, LERONDEL Stéphanie, N'DOYE Oumar, DIAGNE Ibrahim and LE PAPE Alain. 2017. "Modeling and quantifying the detection thresholds of fluorochromes pairedwith a molecular probe of integrins regarding the development of an imaging strategy for the lymph node involvement", *International Journal of Current Research*, 9, (05), 51423-51429.

INTRODUCTION

The concept of sentinel nodes in oncological surgery is based on the fact that the spread of solid tumors in an orderly manner first passes through the lymphatic system. Thus, the sentinel lymph node, the first lymph node encountered by lymphatic drainage from the site of the tumor, is likely to be the first to be affected by metastasis. Therefore, a negative sentinel lymph node makes it very unlikely that other lymph nodes along the same lymphatic pathway will be affected (TORRE, Lindsey, 2015). Based on this hypothesis, morbidity associated with lymph node dissection can be avoided if no malignant cell is observed in this sentinel lymph node. In routine clinical practice, entinel lymph node research uses technetium colloids detected by scintigraphy and surgical probe. In addition, the anatomopathological examination of the excised lymph nodes remains the gold standard in the staging of the tumor's extension. Apart from very costly rapid molecular biology tests (TORRE, Lindsey, 2015 and RUBIO, Doris McGartland, 2010), routine complete histopathological examination requires a delay (4 to 7 days) to state on the lymph node micro-invasion. This waiting time constitutes a limit as the result may modify the surgical care (TROCHIM, 2011). To these shortcomings are added the investment and operating costs of radio isotopic methods and the regulatory constraints of radiation protection. For all these reasons, we are interested in an alternative molecular imaging technique for the detection of the sentinel lymph node and its micro-invasion. The

Corresponding author: **BADIANE S. Moussa,**
Faculty of Health Sciences /University Gaston Berger of Saint-Louis, Senegal

development of a micro-invasion imaging strategy could provide per-operative information without any delay for proper care. In this context, labelled monoclonal antibodies (Mabs) and RGD mimetic molecular probes are prime targets for in vivo imaging (PET, SPECT, MRI, NIRF). This working step that we report is to validate from sample lymph nodes collected ex vivo, the detectability of a fluorochrome paired with a mime RGD within a lymph node. In a translational research approach, we chose healthy sheep lymph nodes as animal model.

MATERIAL AND METHODS

Animals

Healthy sheep lymph nodes were collected ex vivo from the different ganglionic areas. Their order of magnitude was 12, 60 mm in length, 9, 06 mm in width, 5.02 mm thick with an average mass of 0.42 g.

Table 1. Lymph nodes biometrics

Identity of the lymph node	Weight (g)	Length (mm)	Width (mm)	Thickness (mm)
Témoin	0,285	11,08	7,49	3,58
ICG 1/500	0,697	18,24	11,59	5,45
AF750 1/100	0,291	11,44	7,35	5,09
AF750 1/80	0,269	11 ,74	7,96	4,10
AF750 1/60	0,289	9,09	7,03	5,34
AF750 1/30	0,443	13,66	9,28	5,68
CY 5.5 1/40	0,581	12,6	10,87	5 ,73
CY 5.5 1/30	0,402	12,10	9,45	4,74
CY 5.5 1/20	0,478	12,28	9,93	5,17
CY 5.5 1/10	0,536	12,99	9,74	6,06

Reagents

Fluorochromeschosen are CY5.5-RGD, AF750-RGD, and ICG.

Table 2. Wavelength of excitation and emission of fluorochromes

Fluorochromes	Excitation wavelength	Emission wavelength
CY5.5-RGD	675nm	694nm
AF750-RGD	752nm	776nm
ICG	800 nm	> 800nm

Conduct of the study

Injections of fluorochromes were performed directly in the lymph node parenchyma at a rate of 10 µl for each solution per lymph node. The different dilutions injected were validated the day before by the research further to a series of dilution of the minimal threshold of fluorochromes detectable from a volume of 10 µl on a slide.

The following table summarizes the different doses of injected fluorochromes.

Table 3. Different doses of injected fluorochromes Fluorescence Imaging

Fluorochrome and initial concentration	Dilutions	Quantity inserted in the volume of 10µL (mmol)
AF750-RGD 100 mMol /ml	1/100	0,0100
	1/80	0,0125
	1/60	0,0167
	1/30	0,0333
CY 5.5-RGD 10 mMol /ml	1/40	0,0025
	1/30	0,0033
	1/20	0,0050
	1/10	0,0100
ICG 1,6µg /800µl (775g/mol)	1/500	7,7500

Fluorescence Imaging

The parameters of acquisition were as follows:

- Imaging technique: The samples were imaged by Epi-Fluorescence and so as to make "Spectral Unmixing" and "Image Math".
- Binning: Small (2x2) and Medium (4x4)
- Visual range (height of the plateau): B (7,5cm)
- Time of acquisition: 5to 15 seconds
- Different filters have been used according to the fluorochromes:
- RGD-AF750
- Filters: Ex: 745 nm (bp 35 nm) - Em: 800 nm (bp 20 nm) - Auto fluorescence: 535 nm (bp 35 nm)
- Spectral Unmixing at excitation and emission.
- RGD-Cy5.5
- Filters: Ex: 675 nm (bp 35 nm) Em: 720 nm (bp 20 nm) Auto-fluorescence: 500 nm (bp 35 nm)
- Spectral Unmixing at excitation and emission.
- ICG (Indo Cyanine Green)
- Filters: Ex: 745 nm (bp 35 nm) - Em: 840 nm (bp 20 nm) - Auto-fluorescence: 535 nm (bp 35 nm)
- No Spectral Unmixing

RESULTS

Fluorescence by simple pairs of filters:

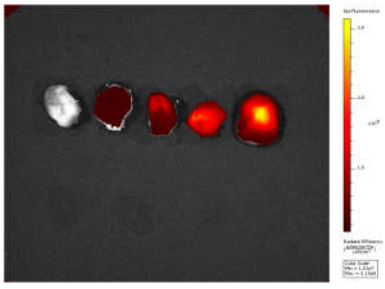

Figure 1. Sheep lymph node AF750 –RGD, RGD-AF750: signal detectable at dilution 1/100

Table 4. Quantification of lymph node fluorescence at different dilutions of RGD-AF750: signal detectable at dilution 1/100

Identification	SampleLN (lymphnode)	LN1/100	LN1/80	LN1/60	LN1/30
Quantification of Radiant efficiency (p/s/cm2/sr)/(µW/cm2)	$1{,}162.10^{7}$	$1{,}68.10^{8}$	$4\ ,163.\ 10^{8}$	$9{,}305.10^{8}$	$1\ ,497.10^{9}$

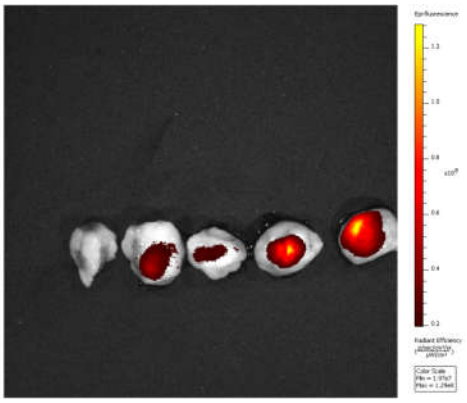

Figure 2. Sheep lymph nodesCY5.5 –RGD, Cy5.5, signal detectable from dilution 1/20

Table 5. Quantification of lymph node fluorescence at different dilution CY5.5 –RGD

Identification	Sample LN (LymphNode)	LN (LYMPH NODE) 1/40	LN1/30	LN1/20	LN1/10
Quantification of Radiant efficiency (p/s/cm2/sr)/(µW/cm2)	$1{,}119\ .10^{8}$	$2{,}616\ .10^{8}$	$1{,}612\ .10^{8}$	$2{,}984.10^{8}$	$4{,}420.10^{8}$

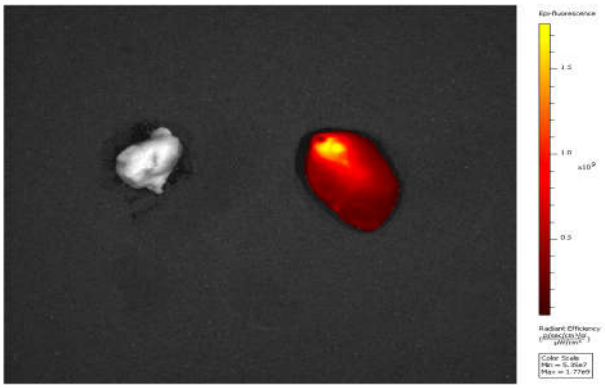

Figure 3. Sheep lymph nodes ICG

Table 6. Quantification of lymph node ICG fluorescence

Identification	SampleLN (LymphNode)	LN (LymphNode) ICG 1/500
Quantification of Radiant efficiency (p/s/cm2/sr)/(µW/cm2)	$1{,}541.10^{8}$	$1{,}269.10^{10}$

Table 7. Quantification of lymph node fluorescence at different dilution CY5.5 –RGD after spectral unmixing (eg 605nm em: 660 to 700)

Identification	Sample LN (LymphNode)	LN (LYMPH NODE)1/40	LN1/30	LN1/20	LN1/10
Quantification of Radiant efficiency (p/s/cm2/sr)/(µW/cm2)	$1{,}67.10^{7}$	$8{,}53\ .10^{7}$	$5{,}21.10^{7}$	$1{,}07.10^{8}$	$1{,}68.10^{8}$
Quantification of Radiant efficiency (p/s/cm2/sr)/(µW/cm2) without correction ex640 em720	$1{,}04.10^{8}$	$1{,}84.10^{8}$	$1{,}15.10^{8}$	$1{,}75.10^{8}$	$2{,}05.10^{8}$

Image processing by spectral unmixing and image math
1st series of acquisition

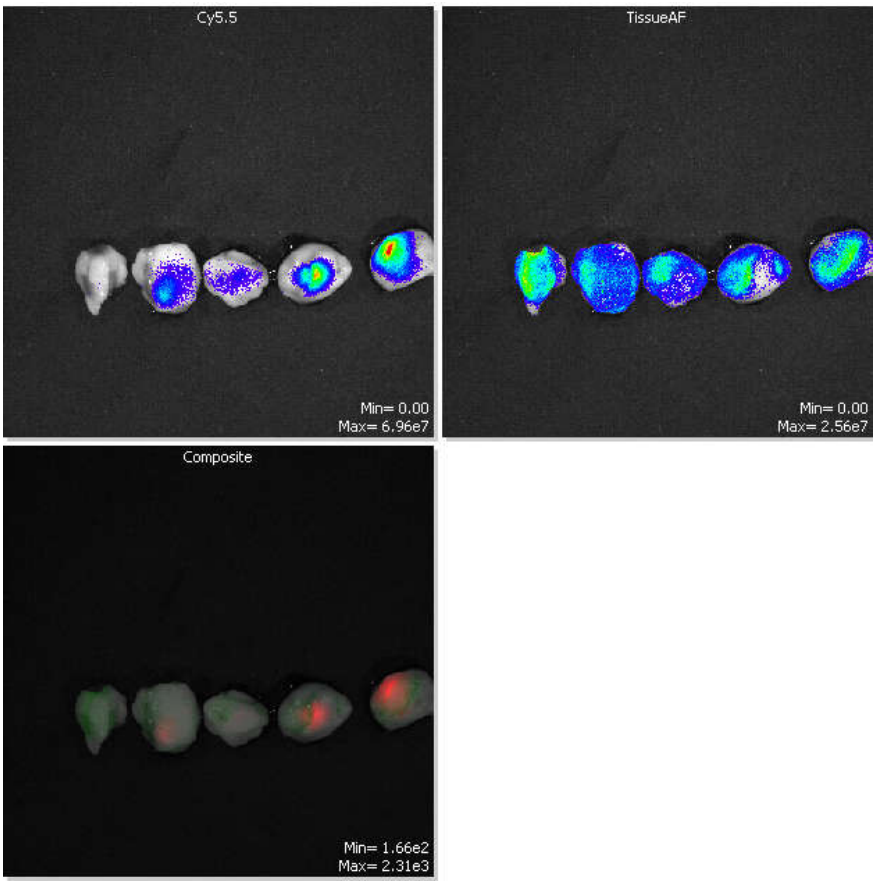

Figure 4. Spectral Unmixing: representation of autofluorescence (eg 605nm em: 660 to 700), probe fluorescence and composite

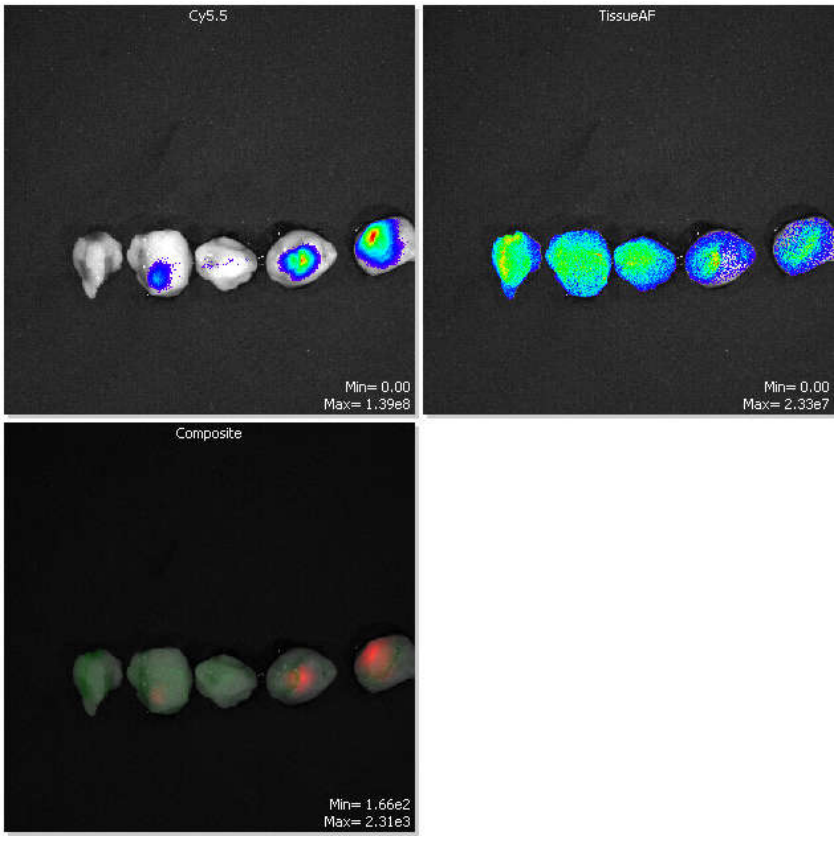

Figure 5. Spectral Unmixing: representation of the fluorescence of Cy5.5 probe(ex: 675nmem: 720 to 780), of autofluorescence and composite.

Table 8. Quantification of lymph node fluorescence at different dilution CY5.5 –RGD after spectral unmixing (ex: 675nm em: 720 to 780), of autofluorescence and composite

Identification	Sample LN (LymphNode)	LN (LYMPH NODE)1/40	LN1/30	LN1/20	LN1/10
Quantification of Radiant efficiency (p/s/cm2/sr)/(µW/cm2)	$9{,}73.10^{6}$	$1{,}13\ .10^{8}$	$6{,}17.10^{7}$	$2{,}31.10^{8}$	$3{,}74.10^{8}$
Quantification of Radiant efficiency (p/s/cm2/sr)/(µW/cm2) Without correction ex675 em720	$1{,}12.10^{8}$	$2{,}62.10^{8}$	$1{,}61.10^{8}$	$2{,}98.10^{8}$	$4{,}42.10^{8}$

2nd series of acquisition

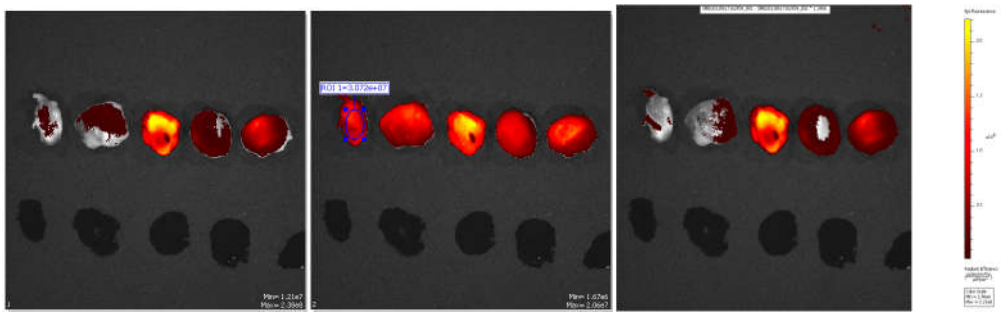

Figure 6. Image Math: Sequence (645/720 then 500/725nm) with the region of interest on the auto-fluorescence and theresults of the subtraction

Table 9. Quantification of lymph node fluorescence at different dilution CY5.5 –RGD after spectral unmixing, Image Math: Sequence (645/720 then 500/725nm) with the region of interest

Identification	Sample LN (LymphNode)	LN (LYMPH NODE)1/40	LN1/30	LN1/20	LN1/10
Quantification of Radiant efficiency (p/s/cm2/sr)/(µW/cm2)	$1{,}91.10^{7}$	$6{,}55\ .10^{7}$	$1{,}37.10^{9}$	$1{,}69.10^{8}$	$5{,}31.10^{8}$
Quantification of Radiant efficiency (p/s/cm2/sr)/(µW/cm2) Without correction ex675 em720	$7.56.10^{7}$	$1{,}02.10^{8}$	$1{,}24.10^{9}$	$1{,}99.10^{8}$	$5{,}81.10^{8}$

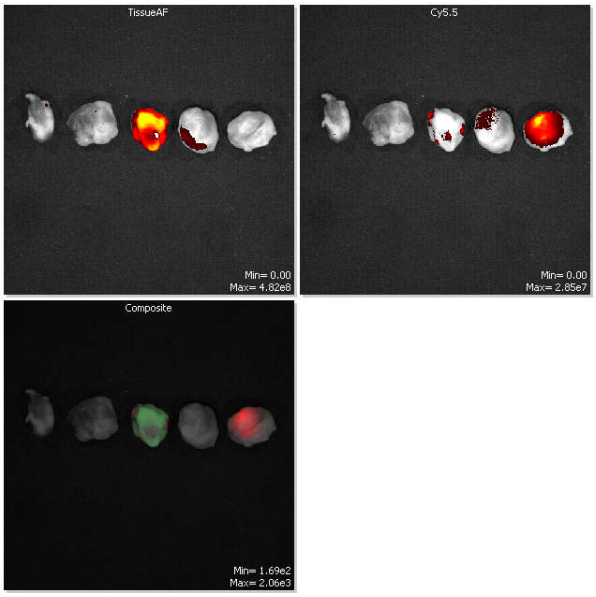

Figure 6. Spectral Unmixing: Sequence (ex: 605nm em: 660 to 700) representation of autofluorescence, andfluorescenceofthe probe and composite

Table 10. Quantification of lymph node fluorescence at different dilution CY5.5 –RGD after Spectral Unmixing: Sequence (ex: 605nm em: 660 to 700)

Identification	Sample LN (LymphNode)	LN (LYMPH NODE)1/40	LN1/30	LN1/20	LN1/10
Quantification of Radiant efficiency (p/s/cm2/sr)/(µW/cm2)	$1{,}84\ .10^{6}$	$7{,}30\ .10^{6}$	$8{,}78\ .10^{6}$	$1{,}79.10^{7}$	$1{,}05.10^{8}$
Quantification of Radiant efficiency (p/s/cm2/sr)/(µW/cm2) Without correction ex605 em660	$1{,}87.10^{8}$	$2{,}49.10^{8}$	$1{,}86.10^{9}$	$2{,}83.10^{8}$	$1{,}95.10^{8}$

For this acquisition, it appears that the lymph node in the central position has a strong autofluorescence. It seems corrected in SPUM but not with the subtraction of background noise.

Specificcomments

The peri-ganglionic fat should be eliminated as much as possible to improve fluorescence and decrease the auto-fluorescence of tissues.

DISCUSSION

The strategy that underpins our targeting approach is based on the affinity between the integrins and the RGD (Yunpeng, 2208). Integrins including heterodimerictransmembrane receptors composed of an α subunit and a β subunit which gather in several combinations (BARCZYK, Malgorzata, 2010). They are prime targets for sensitive and specific molecular imaging in oncology. Integrin αvβ3 is virtually non-existent in the healthy endothelium whereas integrin αvβ5 is expressed at relatively low levels. On the other hand, they are over expressed in activated endothelial cells (BROOKS, 1994) and in a large number of tumor types (Desgrosellier,, 2010) such as glioblastomas (BELLO, Lorenzo, 2001). Melanomas (ALBELDA, 1990), breast cancers (FELDING-HABERMANN. 2001), lung (Wayner,, 1991). [11] andrenal cancers (Rabb, 1996), because tumors are very often derived from endothelial tissue. The expression of the two integrins is not always systematic, only one or the other can be overexpressed bytumor cells (HAFDI, 2000). These two integrins have been intensively researched because they are strongly involved in the process of cancerization, especially in the stages of proliferation (Friedlander, 1995) migration (Kenny, 2008; Ricono, 2009 and RAMSAY, 2007) and cell survival (Stupack, 2005).RGD is the endogenous ligand of theintegrins. It is a peptide sequence formed by the association of the following three amino acids: Arginine-Glycine-Aspartic Acid. The tripeptide pattern is present in many proteins, mostly located in the ECM, such as: fibronectin, vitronectin, osteopontin, collagen, thrombospondin, and fibrinogen (Ruoslahti, 1987). The RGD structure is of great interest for both therapy and diagnostic imaging. In order to increase the affinity and the specificity of interaction of the RGD patterns for their targets, an important research has been carried out on the structure of the RGD as well as on its multimerization (Bogdanowich-Knipp, 1999). In this work, the molecular probe paired with fluorochromes is mime RGD in monomeric form, called S46744. It is a peptidomimetic of the RGD pattern developed by TECHNOLOGIE SERVIER laboratory adapted to specific molecular imaging of integrins. The theoretical and experimental bases of the targeting of integrins αvβ3 and αvβ5 carried out with this probe have been studied on mouse models. The results reported showed good sensitivity according to the fluorescence yield and high specificity on tumor models of heterotopic grafts of cancers expressing the integrins αvβ3 and αvβ5. This suggests that this molecule constitutes a candidate of choice in in vivo tumor targeting, for surgical guidance in the detection and resection of malignant lesions (LEPAPE, 2016).

Thus, the type of fluorochrome associated with S46774 plays a fundamental role, the optical properties being different; hence the advantage of studying the detectability of several fluorochromes paired with the probe at different concentrations in lymph nodes sizing the same as human sentinel lymph node.In our approach, the RGD-AF750 makes it possible to obtain at the 1: 100 dilution a signal/auto-fluorescence ratio sufficient to detect the fluorochrome. 1 lof difference with the sample without fluorescence. At this wavelength the auto-fluorescence is low therefore the image processing is not necessary to improve the contrast. At the wavelength of Cy5.5, visually and in relation to the quantified data, the fluorescent signal can be detected unequivocally from the dilution 1/20. Subtraction of background noise or Spectral Unmixing could improve the detectability threshold. For the ICG, only one concentration was tested and this was sufficient to detect the marker with 2 log difference compared to the sample. The optical properties of ICG vary greatly depending on the medium and the concentration. Our interest in this fluorochrome lies in its diffusibility from the lymphatic system (Tellier, 2010). Through its trapping at the level of the lymph node which is positioned in filter, it allows us to locate the sentinel lymph node. Its fluorescence yield can serve as a benchmark by the long experience of its use in humans.

Conclusions

Near-infrared fluorescence molecular imaging is a non-irradiating modality based on the principle of detection of a wavelength emitted by fluorochromes excited by a non-ionizing light source. In the detection of the sentinel lymph node and its invasion, it is logical to consider the replacement of radioisotopes by fluorochromes paired with a molecular probe for integrin targeting. However, the absorbency of haemoglobin and melanin is not to be obscured on the impact of the signal to be detected. For the different fluorochromes tested, we can retain from this experiment that the AF750-RGD gives good fluorescence signal from the 1/100 dilution, i.e. 10 nmol, and this fluorescence increases with the concentration of AF750-RGD. For the Cy5.5, the net fluorescence signal appears only from the dilution 1/20 i.e. 5 nmol and intensifies with dilution 1/10. Finally, for the ICG, a good fluorescence signal is obtained with respect to the sample at the dilution 1/500, i.e. 7.75 mmol. However the unmixing spectral better than the subtraction of background noise improves the contrast.The validation of these detection thresholds from lymph nodes sizing the same as sentinel lymph nodes in humans gives us guidance on the choice of fluorochromes and their concentration for future explorations.

REFERENCES

Albelda, Steven M., Mette, Stephen A., Elder, David E., *et al*. Integrin distribution in malignant melanoma: association of the β3 subunit with tumor progression. Cancer research, 1990, vol. 50, no 20, p. 6757-6764.

Barczyk, Malgorzata, Carracedo, Sergio, etGullberg, Donald. Integrins. Cell and Tissue research, 2010, vol. 339, no 1, p. 269.

Bello, Lorenzo, Francolini, Maura, Marthyn, Paola, *et al*. αvβ3 and αvβ5 integrin expression in glioma periphery. Neurosurgery, 2001, vol. 49, no 2, p. 380-390.

Bogdanowich-Knipp, Susan J., CHAKRABARTI, Soma, SIAHAAN, Teruna J., *et al*. Solution stability of linear vs. cyclic RGD peptides. Chemical Biology & Drug Design, 1999, vol. 53, no 5, p. 530-541.

Brooks, Peter C., Clark, Richard A., etCheresh, David A. Requirement of vascular integrin alpha-v beta-3 for angiogenesis. Science, 1994, vol. 264, no 5158, p. 569-572.

Desgrosellier, Jay S. etCheresh, David A. Integrins in cancer: biological implications and therapeutic opportunities. Nature Reviews Cancer, 2010, vol. 10, no 1, p. 9-22.

Felding-Habermann, Brunhilde, O'TOOLE, Timothy E., SMITH, Jeffrey W., *et al*. Integrin activation controls metastasis in human breast cancer. Proceedings of the National Academy of Sciences, 2001, vol. 98, no 4, p. 1853-1858.

Friedlander, M., P. C. Brooks, R. W. Shaffer, C. M. Kincaid, J. A. Varner & D. A. Cheresh (1995) Definition Of 2

Angiogenic Pathways By Distinct Alpha(V) Integrins. Science, 270**,** 1500-1502.

Hafdi, Z., Lesavre, P., Nejjari, M., *et al*. Distribution of αvβT3, αvβTB5 Integrins and the Integrin Associated Protein—IAP (CD47) in Human Glomerular Diseases. Cell Communication & Adhesion, 2000, vol. 7, no 6, p. 441-451.

Kenny, H. A., S. Kaur, L. M. Coussens & E. Lengyel, 2008. The initial steps of ovarian cancer cell metastasis are mediated by MMP-2 cleavage of vitronectin and fibronectin. Journal of Clinical Investigation, 118**,** 1367-1379.

Lepape, Alain, Lerondel, Stéphanie, Reveillon, Guillaume, etal. Imaging agents, process for the preparation thereof and pharmaceutical compositions containing same. U.S. Patent No 9,278,143, 8 mars 2016.

Rabb, H., E. BarrosoVicens, R. Adams, J. PowSang& G. Ramirez 1996. Alpha-V/beta-3 and alpha-V/beta-5 integrin distribution in neoplastic kidney. *American Journal of Nephrology*, 16, 402-408.

Ramsay, Alan G., Marshall, John F., et Hart, Ian R. Integrin trafficking and its role in cancer metastasis. Cancer and Metastasis Reviews, 2007, vol. 26, no 3, p. 567-578.

Ricono, J. M., M. Huang, L. A. Barnes, S. K. Lau, S. M. Weis, D. D. Schlaepfer, S. K. Hanks & D. A. Cheresh 2009. Specific Cross-talk between Epidermal Growth Factor Receptor and Integrin alpha(v)beta(5) Promotes Carcinoma Cell Invasion and Metastasis. Cancer Research, 69, 1383-1391.

Rubio, Doris McGartland, Schoenbaum, Ellie E., LEE, Linda S., *et al*. Defining translational research: implications for training. Academic medicine: journal of the Association of American Medical Colleges, 2010, vol. 85, no 3, p. 470.

Ruoslahti, Erkkiet PIERSCHBACHER, Michael D. New perspectives in cell adhesion: RGD and integrins. Science, 1987, vol. 238, no 4826, p. 491-498.

Stupack, Dwayne G. et CHERESH, David A. Get a ligand, get a life: integrins, signaling and cell survival. Journal of cell science, 2002, vol. 115, no 19, p. 3729-3738.

Tellier, Franklin, Ravelo, Rasata, SIMON, Hervé, *et al*. Sentinel lymph node detection by an optical method using scattered photons. Biomedicaloptics express, 2010, vol. 1, no 3, p. 902-910.

Torre, Lindsey A., BRAY, Freddie, SIEGEL, Rebecca L., *et al*. Global cancer statistics, 2012. CA: a cancer journal for clinicians, 2015, vol. 65, no 2, p. 87-108.

Trochim, William, Kane, Cathleen, Graham, Mark J., *et al*. Evaluating translational research: a process marker model. *Clinical and translational science*, 2011, vol. 4, no 3, p. 153-162.

Wayner, E. A., R. A. Orlando & D. A. Cheresh 1991. Integrin-alpha-v-beta-3 and integrin-alpha-v-beta-5 contribute to cell attachment to vitronectin but differentially distribute on the cell-surface. *Journal of Cell Biology*, 113**,** 919-929.

Yunpeng, Y.E., BLOCH, Sharon, XU, Baogang, *et al*. Design, synthesis, and evaluation of near infrared fluorescent multimeric RGD peptides for targeting tumors. *Journal of medicinalchemistry,* 2006, vol. 49, no 7, p. 2268.

****